Disabling *c-Myc* in Childhood Medulloblastoma and Atypical Teratoid/Rhabdoid Tumor Cells by the Potent G-Quadruplex Interactive Agent S2T1-6OTD

Tarek Shalaby[1], André O. von Bueren[1], Marie-Louise Hürlimann[1], Giulio Fiaschetti[1], Deborah Castelletti[1], Tera Masayuki[3], Kazuo Nagasawa[3], Alexandre Arcaro[1], Ilian Jelesarov[2], Kazuo Shin-ya[4], and Michael Grotzer[1]

Abstract

We investigated here the effects of S2T1-6OTD, a novel telomestatin derivative that is synthesized to target G-quadruplex–forming DNA sequences, on a representative panel of human medulloblastoma (MB) and atypical teratoid/rhabdoid (AT/RT) childhood brain cancer cell lines. S2T1-6OTD proved to be a potent *c-Myc* inhibitor through its high-affinity physical interaction with the G-quadruplex structure in the *c-Myc* promoter. Treatment with S2T1-6OTD reduced the mRNA and protein expressions of *c-Myc* and *hTERT*, which is transcriptionally regulated by *c-Myc*, and decreased the activities of both genes. In remarkable contrast to control cells, short-term (72-hour) treatment with S2T1-6OTD resulted in a dose- and time-dependent antiproliferative effect in all MB and AT/RT brain tumor cell lines tested (IC$_{50}$, 0.25–0.39 μmol/L). Under conditions where inhibition of both proliferation and *c-Myc* activity was observed, S2T1-6OTD treatment decreased the protein expression of the cell cycle activator cyclin-dependent kinase 2 and induced cell cycle arrest. Long-term treatment (5 weeks) with nontoxic concentrations of S2T1-6OTD resulted in a time-dependent (mainly *c-Myc*–dependent) telomere shortening. This was accompanied by cell growth arrest starting on day 28 followed by cell senescence and induction of apoptosis on day 35 in all of the five cell lines investigated. On *in vivo* animal testing, S2T1-6OTD may well represent a novel therapeutic strategy for childhood brain tumors. *Mol Cancer Ther; 9(1); 167–79. ©2010 AACR.*

Introduction

Medulloblastomas (MB) are the most common malignant pediatric neoplasms of the central nervous system (CNS) and represent >20% of all pediatric brain tumors (1). With current treatment strategies, nearly half of all patients will eventually die from progressive tumors. CNS atypical teratoid/rhabdoid tumors (AT/RT) are rare but highly malignant embryonal tumors in young children (2–5). Experience to date indicates that infants and children with CNS AT/RT respond very poorly to chemotherapy and radiotherapy (6–9). Accordingly, the identification of novel therapeutic strategies for MB and AT/RT remains a major goal.

Authors' Affiliations: [1]Department of Oncology, University Children's Hospital Zurich; [2]Department of Biochemistry, University of Zurich, Zurich, Switzerland and [3]Department of Biotechnology and Life Science, Tokyo University of Agriculture and Technology; [4]National Institute of Advanced Industrial Science and Technology, Tokyo, Japan

Note: Supplementary materials for this article are available at Molecular Cancer Therapeutics Online (http://mct.aacrjournals.org/).

Corresponding Author: Michael Grotzer, University Children's Hospital Zurich, Steinwiesstrasse 75, 8032 Zurich, Switzerland. Phone: 41-44-266-71-11; Fax: 41-44-266-71-71. E-mail: Michael.Grotzer@kispi.uzh.ch

doi: 10.1158/1535-7163.MCT-09-0586

Telomestatin is a natural G-quadruplex–intercalating agent isolated from *Streptomyces anulatus* 3533-SV4 (10). Telomestatin is a potent telomere maintenance-disabling drug in cervical carcinoma, breast cancer, multiple myeloma, leukemia, and neuroblastoma cells (11–14). Telomestatin suppresses cellular proliferation and induces apoptosis within a few days in various cancer cells but not in normal cells (15). Telomestatin has a characteristic macrocyclic ring system that consists of sequential pentaoxazoles, bismethyloxazoles, and a thiazoline. It has been suggested that these structural features of telomestatin strongly bind to G-quartets by overlapping, and this interaction is believed to promote the formation and stabilization of G-quadruplex structures (16). To increase this interaction, installation of additional functional groups, such as carbonyl, hydroxyl, and/or amino groups, would be required. Based on this concept, telomestatin derivatives were designed, and S2T1-6OTD was synthesized as a derivative bearing a macrocyclic bisamide (15). Based on its three-dimensional structure, it had been speculated that S2T1-6OTD has a high affinity for G-quadruplex–forming sequences, including the nuclease hypersensitivity element III1 (17). This is a major transcriptional control element in the *c-Myc* promoter region, and it has been found to control up to 85% of total *c-Myc* transcription (17–23).

c-Myc is a pleiotropic transcription factor that has been linked to diverse cellular functions, such as cell cycle

regulation (24), proliferation (25), and growth (26), and it has an important regulatory effect on telomerase activity (27, 28) that promotes immortalization. Aberrant *c-Myc* signaling has been observed in human cancers, and *c-Myc* has been shown to promote cell transformation and tumor progression (29–33). In childhood MB, high *c-Myc* mRNA expression and *c-Myc* gene amplification have been suggested as indicators of poor prognosis (33–43). Furthermore, high *c-Myc* mRNA expression was shown to be significantly associated with tumor anaplasia (44, 45).

In this study, we examined the short- and long-term effects of S2T1-6OTD in a representative set of childhood MB and AT/RT cells.

Materials and Methods

Tumor and Control Cells

DAOY human MB cells, CA46 and Ramos human Burkitt's lymphoma cells, PC12 rat pheochromocytoma cells, and MRC-5 human untransformed fibroblast cells were purchased from the American Type Culture Collection. D341 and D425 MB cells were the kind gift of Dr. Henry Friedman (Duke University, Durham, NC). DAOY M2 (c-Myc vector–transfected) human MB cells have been described previously (45). BT-12 and BT-16 human CNS AT/RT cells were the kind gift of Dr. Peter Phillips (The Children's Hospital of Philadelphia, Philadelphia, PA). Rat fibroblast cells HO15.19 [*c-Myc* knockout (−/−)] and TGR-1 *c-Myc* wild-type (rat fibroblast) were the kind gift of Prof. B. Amati (European Institute of Oncology, Milan, Italy). DAOY, D341, and D425 cells were cultured in Richter's zinc option medium/10% fetal bovine serum (FBS; 1% nonessential amino acids were added to the medium for D341 and D425 cells and G418 was added to the medium for DAOY M2 to a concentration of 500 μg/mL). BT-12 and BT-16 cells were cultured in DMEM (with Glutamax)/10% FBS. CA46 and Ramos cells were grown in RPMI 1640 supplemented with 10% FBS. MRC-5 cells were grown in MEM supplemented with 5% FBS. PC12 cells were cultured in complete growth medium with FBS to a final concentration of 2.5% horse serum. HO15.19 and TGR-1 cells were cultured in DMEM with 8% calf serum. BJ foreskin fibroblasts were cultured in DMEM containing 10% iron-supplemented calf serum. All cell cultures were maintained at 37°C in a humidified atmosphere with 5% CO_2. Cell lines that were not purchased from the American Type Culture Collection in 2009 were tested for their authentication by karyotypic analysis using molecular cytogenetic techniques, such as comparative genomic hybridization.

PCR-Stop Assay

PCR-stop assay was done as previously reported (46). Oligonucleotides ss-telo24 d[TTAGGGTTAGGGT-TAGGGTTAGGG], ss-Pu22 d[GAGGGTGGG-GAGGGTGGGGAAG], mutated mut-ss-Pu22 d[GAGGGT*AA*GGAGGGTGGGGAAG], and the complementary sequences of telo24 d[TCTCGTCTTCCCTAA]

(telo24 rev) and ss-Pu22 d[ATCGCTTCTCGTCTTCCC-CA] (ss-Pu22 rev) were used. The chain extension reaction was done in 1× PCR buffer containing 0.2 mmol/L deoxynucleotide triphosphate, 5 units Taq polymerase, 7.5 pmol oligonucleotides, and various concentrations of S2T1-6OTD and telomestatin. The mixtures were incubated in a thermocycler under the following conditions: 94°C for 2 min followed by 30 cycles of 94°C for 20 s, 47°C for 20 s, and 72°C for 20 s. Amplified PCR products were resolved on 12% native polyacrylamide gels in 0.5× Tris-borate EDTA buffer and stained with ethidium bromide. The IC_{50} values were calculated based on the fluorescence intensity scanned with a phosphorimager (Typhoon 8600, Molecular Dynamics).

Circular Dichroism Spectroscopy

Circular dichroism (CD) experiments were carried out with a Jasco J-715 instrument equipped with a computer-controlled water thermostat. Optical path length was 1 mm. The spectra were calculated with J-715 Standard Analysis software (Japan Spectroscopic Co.). Each spectrum was recorded thrice, and the reported spectra represent the average of three scans at 5 nm/min and data pitch 0.2 nm. ss-Pu22 (GAGGGTGGGGAGGGTGGG-GAAG) or ss-Telo24 d[TTAGGG]$_4$ was diluted by Tris buffer (50 mmol/L, pH 7.0) at a concentration of 10 μmol/L. S2T1-6OTD was dissolved with 10 mmol/L stock solution and titrated into the DNA samples at 5 mol equivalent (the 10 mmol/L stock solution of S2T1-6OTD was made up in 10% DMSO–90% water). The DNA strand concentrations were 10 μmol/L, and the CD data are a representation of three averaged scans taken at 25°C. All CD spectra are baseline corrected for signal contributions due to the buffer and for buffer and DMSO for the samples containing S2T1-6OTD. Thermal melting experiments were done using 10 μmol/L of either ss-Pu22–forming or ss-Telo24–forming sequence in the presence of 50 μmol/L S2T1-6OTD in a Tris-HCl buffer (50 mmol/L, pH 7.4), and the ellipticity at 264 nm was monitored on continuous heating at 2°C/min between 20°C and 95°C.

Real-time Quantitative Reverse Transcription-PCR

Isolation of total RNA, cDNA synthesis, and kinetic real-time PCR quantification of *hTERT* and *c-Myc* mRNA were done as previously described (47, 48). Experiments were done in triplicate for each data point. The amount of hTERT and *c-Myc*, normalized to the endogenous control 18S rRNA, was related to the commercially available calibrator human cerebellum (Clontech).

Western Blot Analysis

S2T1-6OTD–treated and control MB and AT/RT cells were washed twice in medium, centrifuged, and lysed in buffer [50 mmol/L Tris (pH 8), 150 mmol/L NaCl, 1% Triton X-100, 1% NP40, 0.1% SDS, 5 mmol/L EDTA] for 20 min on ice followed by centrifugation at 10,000 × *g* for 15 min. The crude lysates were heated for 5 min at

Figure 1. PCR-stop assay products in the presence of increasing concentrations of S2T1-6OTD and either G-quadruplex–forming single-stranded *c-Myc* promoter sequence ss-Pu22 (**A**) or telomeric ssDNA sequence ss-Telo24 oligomer (**B**). **C,** quantification of the band absorbance (fluorescence intensity) by using phosphorimager. *Points,* mean of three independent experiments; *bars,* SD. PCR-inhibitory activities were calculated by the following equation: (intensity of the band in the presence of S2T1-6OTD)/ (intensity of positive control band).
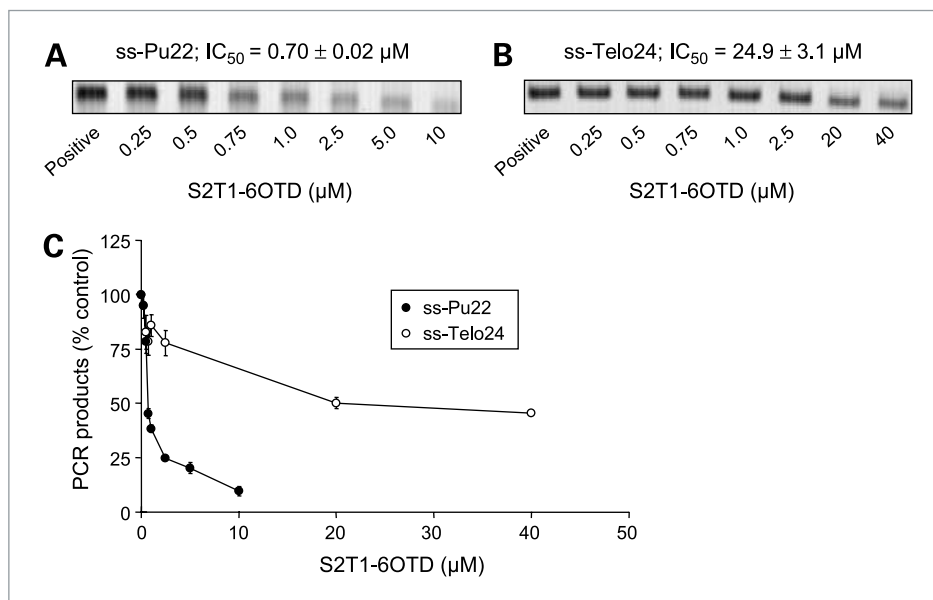
95°C in the presence of 3% mercaptoethanol. Equal amounts of protein (30 μg/lane) from the homogenates were separated by 10% (w/v) SDS-PAGE and transferred onto nitrocellulose membranes (Bio-Rad). Nonspecific binding sites were blocked with 10 mmol/L TBS containing 0.1% Tween 20 and 10% nonfat milk. Membranes were then incubated overnight at 4°C with anti–*c-Myc* monoclonal antibody (Cell Signaling Technology, Inc.), anti–cyclin-dependent kinase 2 (CDK2) monoclonal antibody (Santa Cruz Biotechnology), or anti–β-actin monoclonal antibody (LS2T1-6OTD; Abcam). Membranes were then washed thrice at room temperature, and bound immunoglobulin was detected with anti-isotype monoclonal antibody coupled to horseradish peroxidase (Santa Cruz Biotechnology). The signal was visualized by enhanced chemiluminescence (Amersham Biosciences) and autoradiography. Relative band intensities were determined using Quantity One analysis software (Bio-Rad).

c-Myc Transcription Factor Binding Activation Assay

Nuclear protein extracts were obtained from S2T1-6OTD–treated and S2T1-6OTD–untreated MB and AT/RT cells by using the BD TransFactor Extraction kit (BD Clontech) as described previously (49). The activation of *c-Myc* was measured by using the Mercury TransFactor assay (BD Clontech), an ELISA-based assay (50), as described previously (49).

Cell Cycle Analysis

MB and AT/RT cells were washed with PBS, fixed in 70% ethanol, and kept at −20°C for at least 24 h. They were then washed in PBS and resuspended in 50 mg/mL propidium iodide and RNase (10 mg/mL) in PBS. The cell suspension was incubated for 30 min at room temperature, and cell cycle distribution was determined by

flow cytometry (FACSCalibur, Becton Dickinson), with CellQuest software analysis and quantification using ModFit software as described previously (49).

Cell Growth Assays

For long-term cell growth studies, cells were seeded at 1×10^4/mL (5 mL) into a 25-cm² tissue culture flask in the presence or absence of subtoxic doses of S2T1-6OTD. Subtoxic dose was defined as the concentration inhibiting a maximum of 10% human MB cells grown on a 72-h drug exposure. Cells were then cultured for 4 d and then trypsinized and counted. At each passage, 1×10^4 cells/mL were replated into a new culture flask with fresh medium containing drug solution. Results were expressed as the cumulated population doublings as a function of the time of culture, as described by Binz et al. (14) and Riou et al. (51). For cytotoxicity assay, cell viability was quantified using a colorimetric MTS assay (Promega) as previously described (47, 52). Each condition was done in triplicate.

Telomerase Activity

Telomerase activity in human MB and AT/RT cell lines was measured by using the TeloTAGGG Telomerase PCR ELISA kit (Roche Diagnostics) as previously described (14, 47). All samples were assayed in triplicate.

Telomere Length

Telomere length in MB and AT/RT cells was determined by using the TeloTAGGG Telomere Length Assay (Roche Diagnostics) for measuring the length of telomere restriction fragments as previously described (47).

Apoptosis Assay

A photometric enzyme immunoassay (Cell Death Detection ELISA, Roche Diagnostics) was used for the
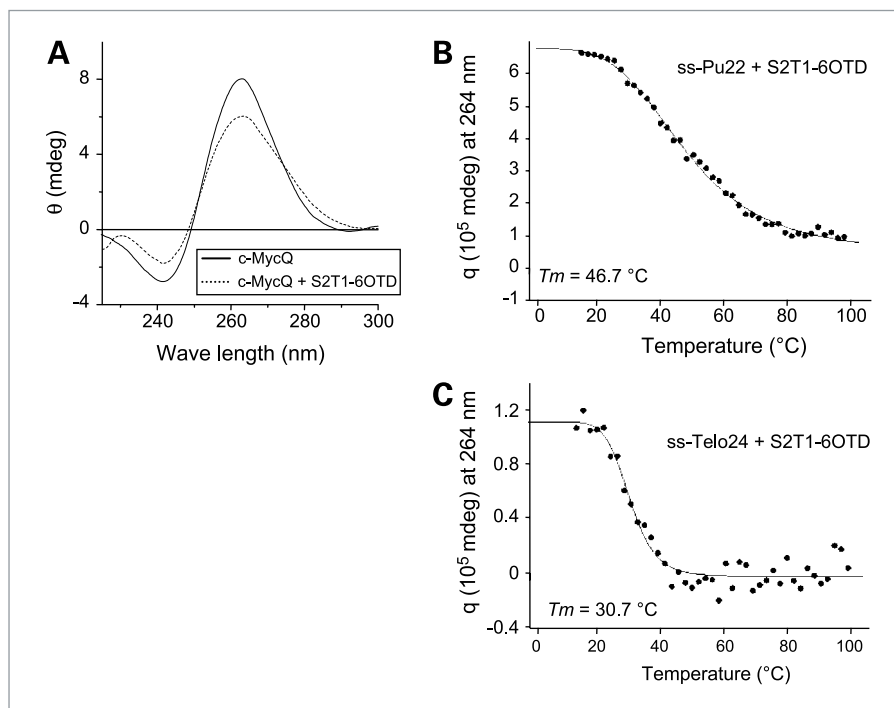
Figure 2. **A,** CD spectra of c-MycQ in the presence or absence of S2T1-6OTD (50 μmol/L). The c-MycQ–forming oligonucleotide concentration was 10 μmol/L. Spectra were recorded in 50 mmol/L Tris (pH 7.2) and 100 mmol/L KCl at 25°C. **B,** CD melting curves of ss-Pu22 (10 μmol/L) at 265 nm in the presence of S2T1-6OTD (50 μmol/L). **C,** CD melting curves of ss-Telo24 (10 μmol/L) at 265 nm in the presence of S2T1-6OTD (50 μmol/L).

quantitative determination of cytoplasmic histone-associated DNA fragments, as described previously (53).

Statistical Analysis

All data are expressed as mean ± SD. Student's t test was used to test statistical significance. $P < 0.05$ was considered to be significant. GraphPad Prism 4 (GraphPad Software) software was used to calculate IC_{50} values and their 95% confidence intervals and to statistically compare the fitted midpoints (log IC_{50}) of the two curves.

Results

S2T1-6OTD Structure

Supplementary Fig. S1A shows the chemical structure of S2T1-6OTD compared with the well-characterized telomestatin. The structure of S2T1-6OTD was confirmed by ^{1}H nuclear magnetic resonance (Supplementary Fig. S1B) and high-resolution mass spectrometry (Supplementary Fig. S1C).

### Stabilization of *c-Myc* G-Quadruplex Structures by S2T1-6OTD

To test whether S2T1-6OTD is able to stabilize the *c-Myc* G-quadruplex in the guanine-rich sequence of the *c-Myc* promoter, we used PCR-stop assay (54). In the presence of increasing concentrations of S2T1-6OTD, the 5′ to 3′ DNA extension of the ssDNA of the *c-Myc* promoter sequence ss-Pu22 oligomer was inhibited in a dose-dependent manner, indicating the stabilization of the G-quadruplex structure by S2T1-6OTD with a low

IC_{50} value of 0.70 ± 0.02 μmol/L (Fig. 1A). No significant inhibition was observed when ss-Pu22 mutant (containing a mutation in two guanine repeats into aniline) was used (data not shown).

Because potential G-quadruplex–forming sequences exist not only in the *c-Myc* promoter region but also in the telomeric ssDNA that proved to be recognized and specifically stabilized by telomestatin, the parental compound of S2T1-6OTD (10), we investigated the selectivity of S2T1-6OTD to stabilize the G-quadruplex in the *c-Myc* promoter ss-Pu22 over the telomeric ssDNA sequence ss-Telo24 by the PCR-stop assay. The results showed that inhibition of ss-Telo24 fragment extension needed a 35-fold higher concentration of S2T1-6OTD (IC_{50}, 24.9 ± 3.1 μmol/L) compared with ss-Pu22 (IC_{50}, 0.70 ± 0.02 μmol/L; Fig. 1B and C), indicating much weaker binding and stabilization ability to G-quadruplex in ss-Telo24 than in ss-Pu22. This result was supported by CD spectroscopy, which showed that S2T1-6OTD failed to stabilize the conformation of ss-Telo24 to a G-quadruplex (Supplementary Fig. S2). Together, these results show a higher selectivity of S2T1-6OTD for the *c-Myc* promoter sequence compared with telomere DNA.

The binding affinity of S2T1-6OTD and stabilization of the G-quadruplex in the *c-Myc* promoter (c-MycQ) were further investigated by CD spectroscopy. Figure 2A shows that, under our experimental conditions, the *c-Myc* G-quadruplex–forming sequence exhibited the typical spectral signature of a G-quadruplex with a characteristic maximum at 264 nm (55, 56). In the presence of a five-times molar excess of S2T1-6OTD, the peak centered at 264 nm was significantly broader, with lower ellipticity

Figure 3. **A,** treatment with S2T1-6OTD results in a reduction of *c-Myc* mRNA as measured by quantitative real-time PCR (*n* = 3) and in a reduction of *c-Myc* protein expression (representative of two independent experiments) in D341, D425, BT-12, and BT-16 cells but not in DAOY cells. *Bars,* SD. **B,** treatment with S2T1-6OTD results in a significant reduction of *c-Myc* activity (measured by *c-Myc* binding capacity to its consensus sequence "CACGTG" of the E-box element) as determined by the ELISA-based TransAM *c-Myc* activity assay. *Columns,* mean absorbance (*n* = 3); *bars,* SD. *, $P < 0.05$; ***, $P < 0.001$. Treatment of MB and AT/RT cells with S2T1-6OTD resulted in a significant decrease of *hTERT* mRNA expression (**C**) and telomerase activity (**D**) as determined by quantitative real-time PCR and the Telomerase PCR ELISA kit. *Columns,* mean percentage decrease compared with untreated control cells (*n* = 3); *bars,* SD.
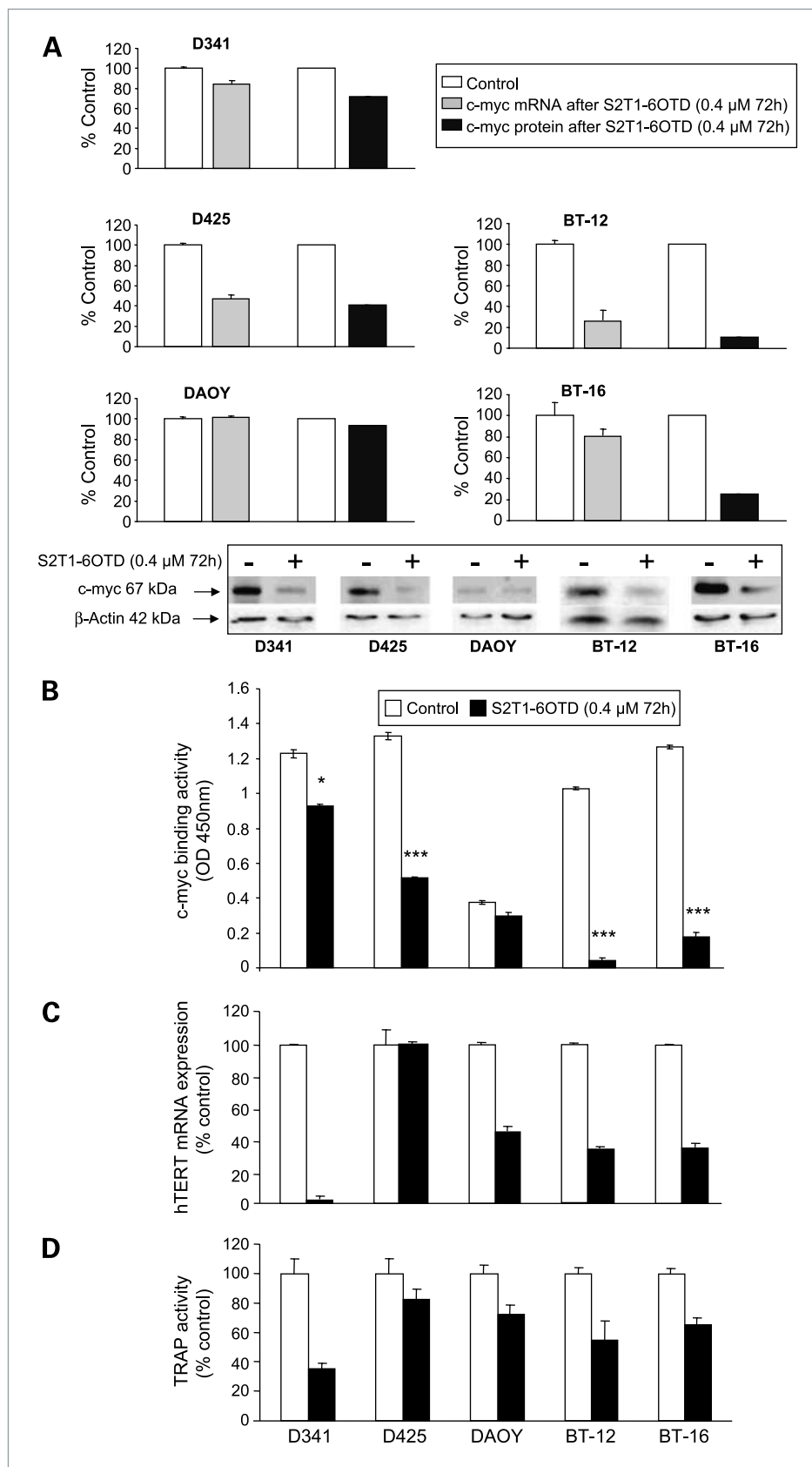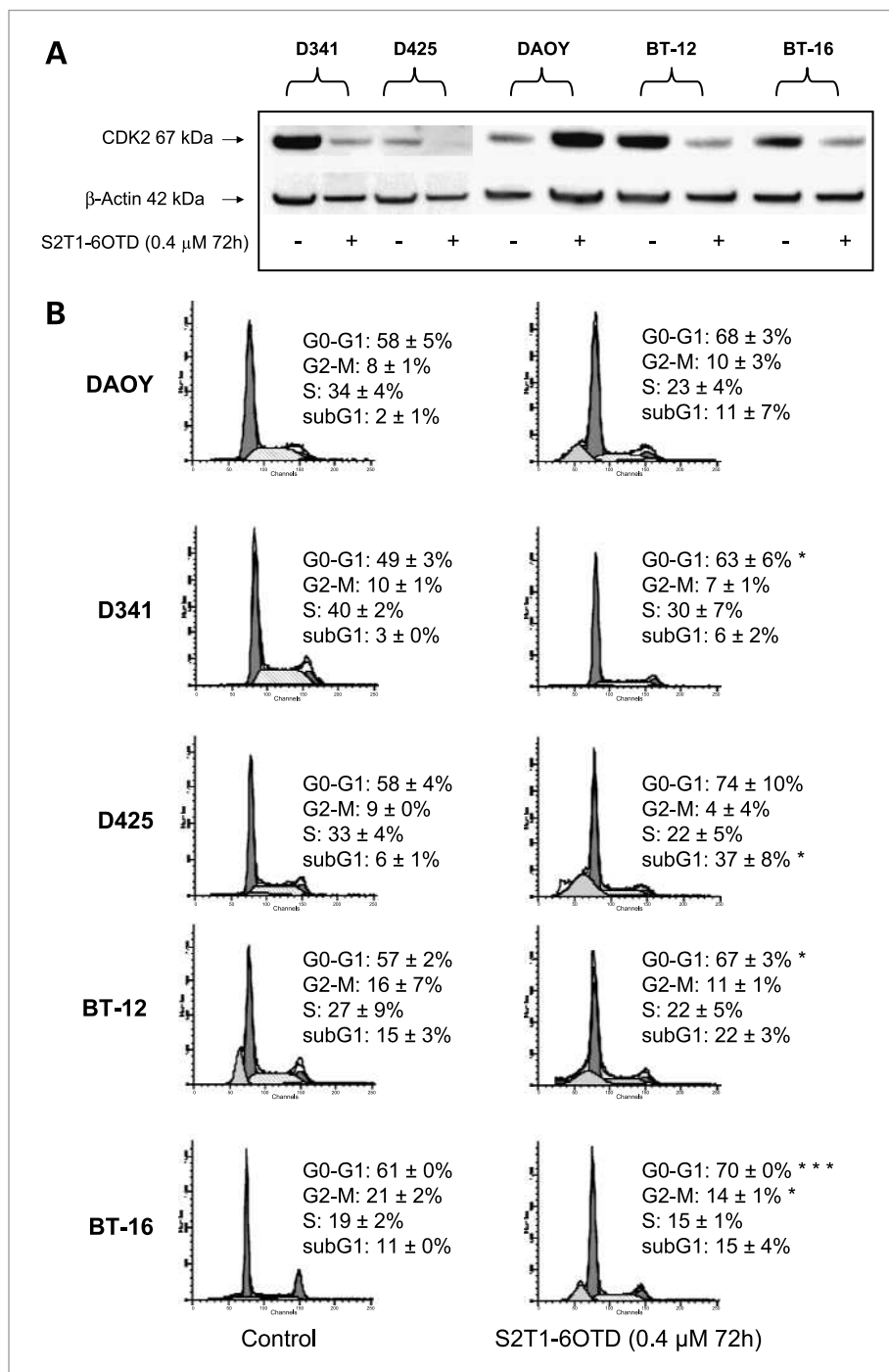
Figure 4. S2T1-6OTD reduces the protein expression of CDK2 and induces cell cycle arrest and apoptotic cell death in human MB and AT/RT cells. **A,** S2T1-6OTD decreased the cell cycle activator CDK2 protein expression in D341, D425, BT-12, and BT-16 but not in DAOY cells as determined by Western blotting. **B,** effects of S2T1-6OTD on cell cycle in human brain tumor cells as determined by fluorescence-activated cell sorting analysis. Cells were treated with S2T1-6OTD (0.4 μmol/L) or left untreated for 72 h and then fixed and stained as described in Materials and Methods. At least 20,000 cells were counted. Results are presented as percentages of cells in G_1, S, G_2-M, and sub-G_1 phases in two independent experiments. The subdiploid peak represents the apoptotic fraction. S2T1-6OTD treatment resulted in a decrease in the percentage of cells in the S phase and an increase in the cells in the G_0-G_1 and sub-G_1 phases in all cell lines tested. *, $P < 0.05$; ***, $P < 0.001$.

at the maximum. This indicates a physical interaction between S2T1-6OTD and the ssDNA of the *c-Myc* promoter sequence. However, the spectral differences were not large enough to permit titration experiments to calculate the binding constant.

Thermodynamic stability profiling provides information about the relative stability of DNA structures on ligand binding (57). Therefore, the stabilization effect of S2T1-6OTD on the G-quadruplex structure in the *c-Myc*

promoter sequence was further studied by CD spectroscopy by measuring the thermodynamic stability profile of the ss-Pu22 oligomer and the change in absorption at 264 nm. The results in Fig. 2B show that the normalized CD intensity of ss-Pu22 at 264 nm with 50 μmol/L S2T1-6OTD in a Tris-HCl buffer (50 mmol/L, pH 7.4) had a T_m value of 46.7°C calculated from the CD melting curves at 264 nm using a sigmoidal fitting. Under the same conditions, the T_m value of S2T1-6OTD-Telo24 complex was

only 30.7°C (Fig. 2C), indicating a strong stabilizing effect of S2T1-6OTD on G-quadruplex in NHE III1 DNA and a weaker effect on G-quadruplex in telomere sequence.

Because indiscriminate binding of a compound to nonspecific DNA can result in significant loss of the compound and may have unintentional effects on the regulation of nontargeted genes, we investigated the binding ability of S2T1-6OTD to duplex DNA. A CD melting curve was done for the duplex ds-Pu22 in the presence or absence of 50 µmol/L S2T1-6OTD. The results showed no detectable change in melting temperature of the ds-Pu22 DNA in the presence or absence of S2T1-6OTD (Supplementary Fig. S3A), indicating the inability of S2T1-6OTD to bind to duplex DNAs. This result was confirmed by the electrophoretic mobility shift assay, which excluded the ability of S2T1-6OTD to interact with dsDNA sequences (Supplementary Fig. S3B).

S2T1-6OTD Treatment Down-Regulates *c-Myc* Expression and *c-Myc* Binding Activity

To test whether treatment with S2T1-6OTD alters c-Myc expression, we incubated a panel of MB and AT/RT cells with 0.4 µmol/L S2T1-6OTD for 72 hours and measured *c-Myc* mRNA expression by real-time quantitative reverse transcription-PCR and *c-Myc* protein by Western blotting. With the exception of DAOY cells (low basal *c-Myc* expression), treatment with S2T1-6OTD resulted in significant reductions of *c-Myc* mRNA and protein expression in all other MB and AT/RT cell lines tested (Fig. 3A). To examine whether treatment with S2T1-6OTD alters *c-Myc* binding activity, we incubated the five cell lines under study with S2T1-6OTD (0.4 µmol/L for 72 hours) and measured binding activity. S2T1-6OTD treatment reduced *c-Myc* binding activity significantly in all MB and AT/RT cells (Fig. 3B).

S2T1-6OTD Reduces Telomerase mRNA Expression and Activity

Because *hTERT*, the catalytic subunit of telomerase, is transcriptionally under the control of *c-Myc* (27, 28) and having shown an inhibitory effect of S2T1-6OTD on *c-Myc* expression in MB and AT/RT cells, we were interested in the effects that this interaction might have on telomerase activity. MB and AT/RT cells were treated with 0.4 µmol/L S2T1-6OTD for 72 hours, total RNA was isolated for reverse transcription-PCR, and total protein was extracted. Using real-time quantitative reverse transcription-PCR to measure *hTERT* mRNA and the Telomerase PCR ELISA kit to measure telomere repeat amplification protocol (TRAP) activity, it was found that S2T1-6OTD could indeed reduce *hTERT* mRNA expression in BT-12, BT-16, DAOY, and D341 cells. No effect was observed on *hTERT* mRNA in the mainly ALT (Alternative Lengthening of Telomeres)-dependent D425 cell line (Fig. 3C; ref. 47). Moreover, S2T1-6OTD reduced telomerase activity in all cell lines tested, with maximum inhibition in D341 (64%) and a minimum 17% in D425 (Fig. 3D).

The direct effect of S2T1-6OTD on telomerase activity was examined in a cell-free system. In this experiment, increasing concentrations of S2T1-6OTD (0.005–5 µmol/L) were added to the telomerase reaction mixture containing extract from D341 cells. The results showed that S2T1-6OTD inhibited *in vitro* the process of telomerase activity; the concentration that resulted in 50% decrease in telomerase inhibition (EC_{50}) was 0.1651 µmol/L when measured by TRAP and was 0.3577 µmol/L when measured by the TRAP-LIG assay (58), which was used to eliminate drug contamination of the PCR reaction. The results of these two experiments not only indicates that S2T1-6OTD by itself has no significant inhibitory effect on the PCR but also confirms that S2T1-6OTD possesses a direct effect on telomerase activity when examined in cell-free system (data not shown).

### NHE III1 Sequence in the Promoter Region of *c-Myc* Is Needed for S2T1-6OTD to Exert Its Effect on *c-Myc*

To further confirm the requirement of the G-quadruplex–forming NHE III1 sequence in the promoter region of *c-Myc* for the exertion of downregulation of *c-Myc* expression by S2T1-6OTD, two Burkitt's lymphoma cell lines with different translocation break points within the *c-Myc* promoter (17, 59, 60) were investigated (Supplementary Fig. S4A). In the CA46 cells where the NHE III1 is deleted, S2T1-6OTD treatment (0.4 and 0.8 µmol/L for 72 hours) had no effect on *c-Myc* mRNA and protein expression, whereas in the Ramos cells, in which the NHE III1 is present, treatment with S2T1-6OTD significantly reduced *c-Myc* mRNA and protein expression (Supplementary Fig. S4B and C). In DAOY M2 MB cells where *c-Myc* is mainly under the control of a cytomegalovirus promoter (45), treatment with S2T1-6OTD did not decrease but rather slightly increased *c-Myc* expression (Supplementary Fig. S4D), also indicating a high affinity of S2T1-6OTD for NHE III1.

Effects of S2T1-6OTD on the Cell Cycle of MB and AT/RT Cells

To determine the possible effects of S2T1-6OTD on cell cycle regulation, we assessed the cellular DNA content by using flow cytometry (fluorescence-activated cell sorting) and determined CDK2 protein expression. With the exception of DAOY cells, S2T1-6OTD (0.4 µmol/L) treatment for 72 hours resulted in a significant decrease in the cell cycle activator CDK2 (Fig. 4A). Moreover, treatment with S2T1-6OTD resulted in a significant decrease in the percentage of cells that were able to enter the S phase and in an increase of the cells in the G_0-G_1 and sub-G_1 phases (Fig. 4B), indicating that S2T1-6OTD mediates cell cycle arrest and induction of apoptotic cell death.

S2T1-6OTD Treatment Results in Suppression of MB and AT/RT Cell Proliferation

To test whether treatment with S2T1-6OTD alters cellular proliferation, MB and AT/RT cells were incubated
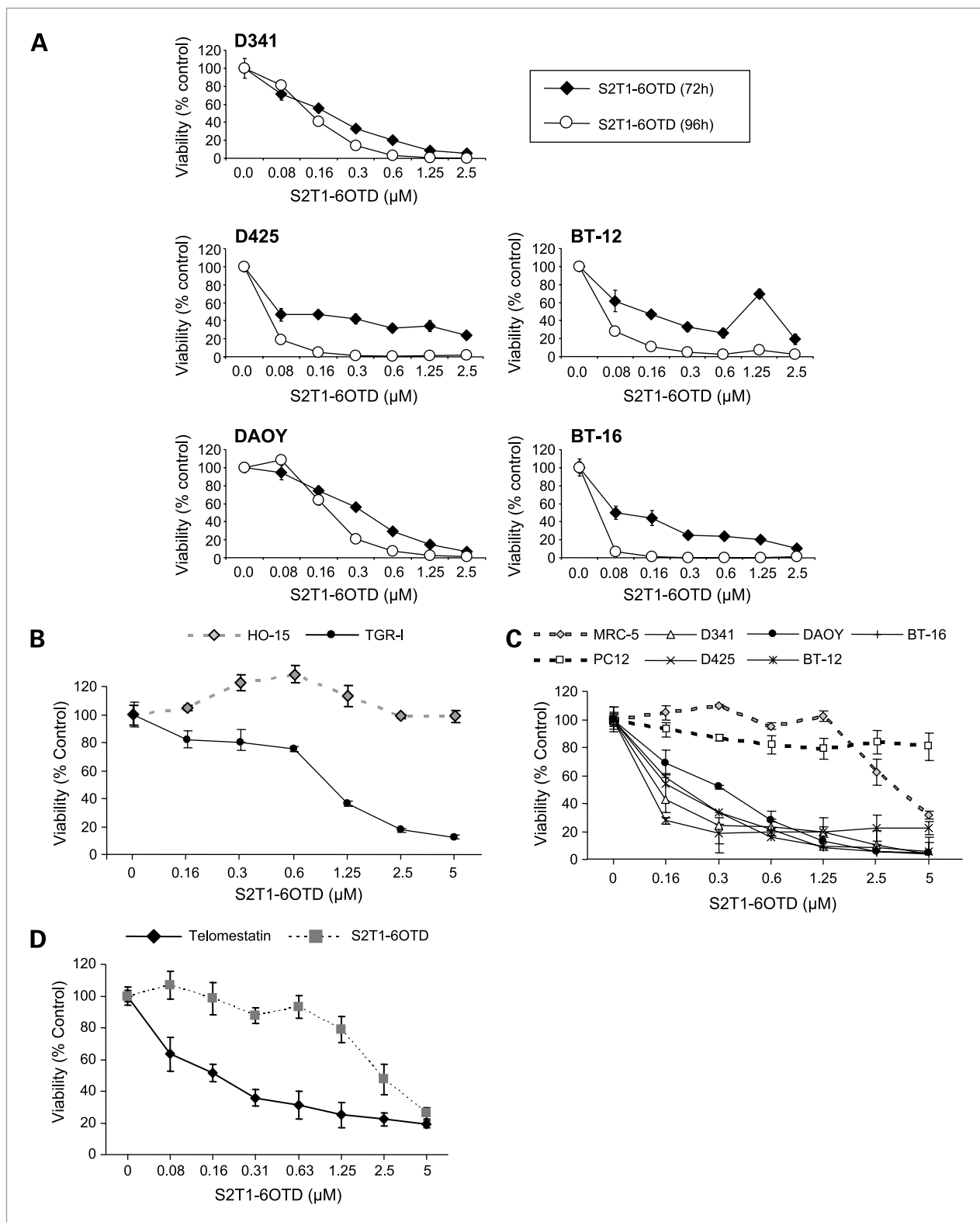
Figure 5. **A,** dose- and time-dependent inhibition of cell viability in MB and AT/RT cells by S2T1-6OTD as determined by MTS assay. **B,** S2T1-6OTD treatment had no antiproliferative effect on HO15.19 [*c-Myc* knockout (–/–)] rat fibroblast cells when compared with the parental TGR-1 *c-Myc* wild-type (rat fibroblast) cells. **C,** S2T1-6OTD treatment also had no major antiproliferative effect on PC12 cells (that do not depend on *c-Myc* in their proliferation) or MRC-5 normal fetal lung fibroblast cells when compared with MB and AT/RT cells. **D,** S2T1-6OTD exhibits much less cell toxicity than telomestatin on MRC-5.

with various concentrations of S2T1-6OTD for 72 or 96 hours and cell viability was assessed by using the MTS assay (Fig. 5A). Treatment with S2T1-6OTD resulted in a dose- and time-dependent cytotoxic response in all cell lines tested, with IC_{50} concentrations between 0.14 and 0.33 μmol/L (72-hour treatment time). However, S2T1-6OTD had no antiproliferative effect on *c-Myc* knockout (−/−) HO15.19 rat fibroblast cells when compared with the parental TGR-1 *c-Myc* wild-type (rat fibroblast) cells (Fig. 5B; ref. 61). Moreover, S2T1-6OTD also had no antiproliferative effect on PC12 cells. These cells do not depend on *c-Myc* to proliferate due to the absence of Max, the partner protein to which *c-Myc* dimerizes to be activated (Fig. 5C; ref. 62). When compared with brain tumor cells, S2T1-6OTD showed significantly less cytotoxic effects (IC_{50}, 3.44 μmol/L) on normal (not transformed) fetal lung fibroblast MRC-5 cells (63, 64), indicating some tumor specificity. Interestingly, when compared with the parental compound telomestatin, S2T1-6OTD showed much less cell toxicity on MRC-5 cells (Fig. 5D). Because S2T1-6OTD also causes a decrease in *hTERT* expression and activity, we investigated whether it was the *c-Myc* downregulation or the reduction in telomerase that exerted the antiproliferative effect of S2T1-6OTD on MB cell culture. To that end, we tested the effect of S2T1-6OTD on cell viability of telomerase-negative cells (e.g., the human foreskin fibroblasts BJ; ref. 65). Treatment with S2T1-6OTD resulted in a clear concentration- and time-dependent cytotoxic response in the telomerase-negative BJ cells (data not shown), indicating that telomerase is most likely not responsible for the effect of S2T1-6OTD on MB and AT/RT cell growth.

Effects of Long-term Treatment with Nontoxic Concentration of S2T1-6OTD

To examine the long-term effects of S2T1-6OTD on MB and AT/RT cells, cells were treated with nontoxic concentrations of S2T1-6OTD (0.04 or 0.004 μmol/L) for 5 weeks. We then characterized the growth properties of the treated cells during the long-term cultivation experiments. Treatment with S2T1-6OTD at 0.04 μmol/L resulted in telomere shortening in all MB and AT/RT cells tested (Fig. 6A). The shortening observed after 3 weeks of S2T1-6OTD treatment was 2.0 kbp in DAOY cells, 1.5 kbp in D341 cells, 2.6 kbp in BT-12 cells, 2.0 kbp in BT-16 cells, but only 0.8 kbp in D425 cells. The growth kinetics of S2T1-6OTD–treated MB and AT/RT cells did not differ significantly from those of untreated control cells in the first week. After 2 to 3 weeks, cell growth of S2T1-6OTD–treated cells decreased (Fig. 6B). Cells treated with S2T1-6OTD at 0.004 μmol/L were able to grow better as compared with cells treated with S2T1-6OTD at 0.04 μmol/L, but a decrease in cell growth was also observed with the very low concentration. The morphologic examination of the 0.04 μmol/L S2T1-6OTD–treated cells at the plateau phase showed an increased proportion of flat and giant cells with phenotypic characteristics of senescence and positive for

senescence-associated β-galactosidase (data not shown). Finally, the cells underwent delayed apoptosis when examined morphologically (data not shown) and were characterized by an increase in apoptotic cell death, as measured by Cell Death Detection ELISA (Fig. 6C).

Discussion

In this study, we investigated the efficiency of S2T1-6OTD to stabilize G-quadruplexes in guanine-rich DNA and examined the strength of its selectivity for the *c-Myc* over the telomeric sequences. We then examined the S2T1-6OTD–mediated cellular effects in a representative set of childhood MB and AT/RT cells.

We have shown here that S2T1-6OTD binds more selectively with higher affinity to the G-quadruplex–forming sequence in the major transcription control element in the *c-Myc* promoter than to the telomeric DNA sequence. This high-affinity physical interaction was established by the results obtained from the PCR-stop assay, which showed that a 35-fold higher concentration of S2T1-6OTD is needed to stabilize a G-quadruplex structure in ss-Telo24 compared with ss-Pu22 sequence. This result was further confirmed by the CD spectroscopy experiments, which showed that the G-quadruplex structure stabilization by S2T1-6OTD in the *c-Myc* promoter tolerated a higher thermal melting point compared with the telomeric DNA sequence.

The preference of a compound for quadruplexes over duplex DNA is of great importance. This is because indiscriminate binding to a duplex DNA can result in a significant loss of the compound and might lead to unexpected cytotoxicity. Our results illustrated that S2T1-6OTD is unable to bind DNA duplexes, as shown by the absence of any changes in the thermal melting curve in the presence of S2T1-6OTD, compared with T_m of naked duplex DNA, rendering it suitable for further studies as a highly selective G-quadruplex–interacting molecule.

Through its ability to recognize and stabilize the quadruplex structure in the *c-Myc* promoter sequence, S2T1-6OTD was able to suppress both *c-Myc* mRNA and protein expression and reduce *c-Myc* activity in MB and AT/RT cell lines after 72-hour incubation; however, the ability to repress *c-Myc* expression was found to be cell type specific. Interestingly, when we treated MB DAOY M2 cells overexpressing *c-Myc* under a different promoter, S2T1-6OTD failed to downregulate c-Myc, indicating specific affinity to the transcriptional control element sequence NHE III1 in the *c-Myc* promoter. In agreement with this was our finding that S2T1-6OTD had no effect on *c-Myc* expression in Burkitt's lymphoma cell line CA46 with the deleted NHE III1 element due to its chromosomal aberration. These results therefore provided convincing evidence that the effect of S2T1-6OTD on *c-Myc* is indeed mediated through the interaction with the *c-Myc* promoter and further implicated effects on *c-Myc*–dependent downstream pathways. However, it has to be said that mechanisms regulating *c-Myc* transcription are multifaceted and involve
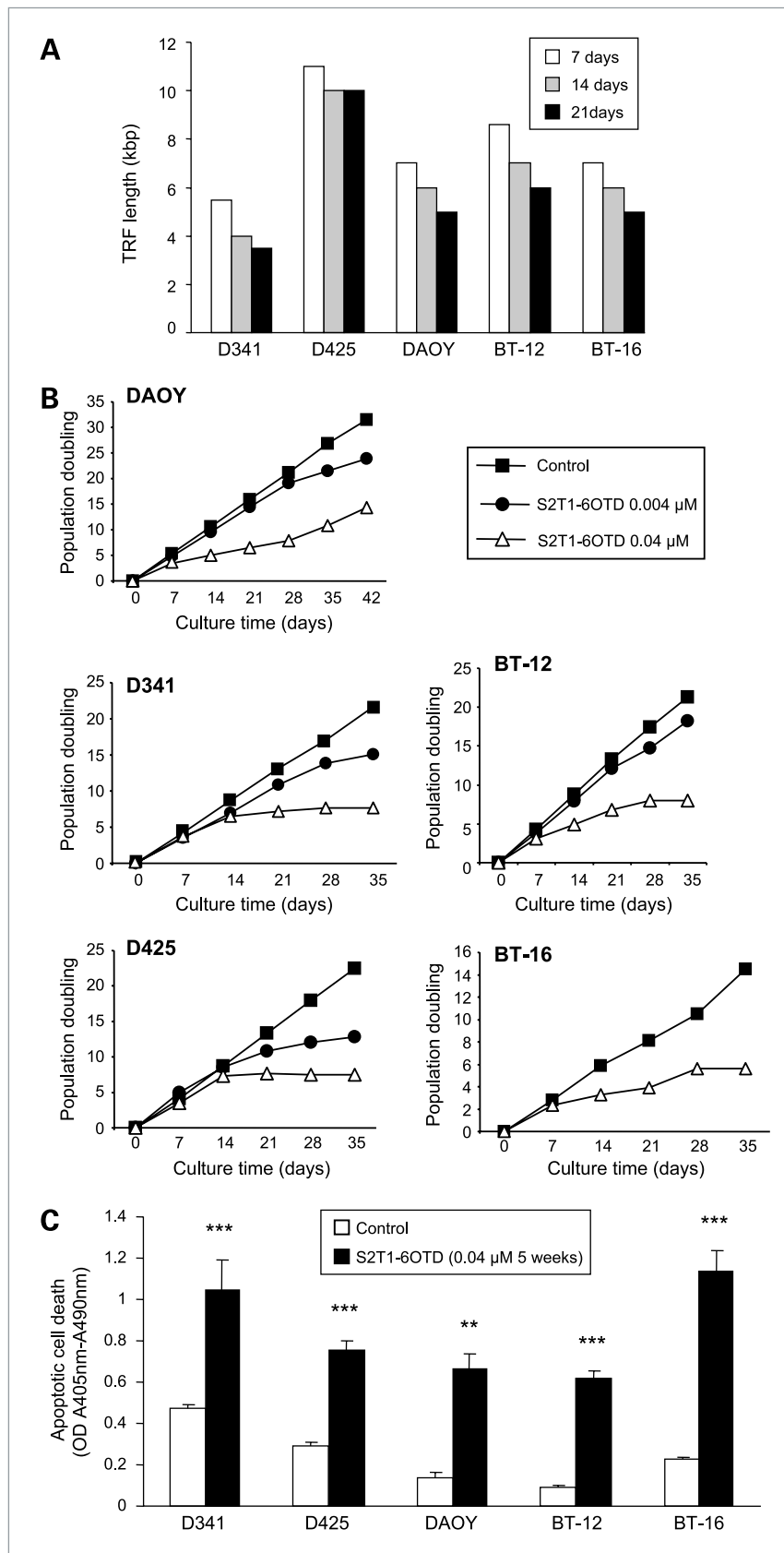
Figure 6. Effects of long-term treatments with nontoxic concentrations of S2T1-6OTD. Every 5 d, the cells were trypsinized and living cells were reseeded at the same number. **A,** effect of 0.04 μmol/L S2T1-6OTD on telomere length as determined by the TeloTAGGG Telomere Length Assay. All cell lines tested showed time-dependent telomere shortening. **B,** effect of 0.04 or 0.004 μmol/L S2T1-6OTD on cell growth as determined by MTS assay. All cell lines tested showed time-dependent decrease in cell growth. **C,** apoptotic cell death was quantified using Cell Death Detection ELISA measuring DNA fragmentation in S2T1-6OTD–treated cells (0.04 μmol/L, for 5 wk). *Columns,* mean absorbance of cytoplasmic histone-associated DNA fragments ($n = 3$; representative of two independent experiments); *bars,* SD. **, $P < 0.005$; ***, $P < 0.001$.

not only the regulatory DNA sequence in *c-Myc* promoter but also several DNA binding proteins that have been shown to preferentially bind to, stabilize, unwind, or cleave the *c-Myc* G-quadruplex structure (66–68). In addition, recent reports have shown that putative G-quadruplex sequences are widespread in >40% of human gene promoters (66, 67). Hence, it could be speculated that any mutation in the regulatory motifs, differences in DNA binding protein expression patterns, or off-target ligand interaction might be critical for the sensitivity toward G-quadruplex–based *c-Myc* inhibitor, such as S2T1-6OTD, in some cell lines, and their effect might present a different profile of biological activity than initially expected.

Based on previously published work, it is well established that the suppression of *c-Myc* expression is closely linked to the specific arrest in the G_0-G_1 cell cycle phase (69–72) and downregulation of *c-Myc* inhibits both cyclins and CDK2 expression in rhabdomyosarcoma (73), in T lymphocytes (74), and in colorectal cancer cells (75). Our results show that under the conditions where inhibition of both proliferation and *c-Myc* activity was observed, S2T1-6OTD treatment resulted in a decrease in the protein expression of the cell cycle activator CDK2 and in a clear G_0-G_1 cell cycle arrest in all brain tumor cell lines tested and decreased the percentage of the cells that were able to enter the S phase. This provided additional evidence that *c-Myc* must be a direct target for S2T1-6OTD action. However, it is noteworthy that S2T1-6OTD was able to induce cell cycle arrest despite no measurable decrease in the mRNA/protein level of *c-Myc* was observed in DAOY cells after 72-hour treatment. These results suggest that inhibition of *c-Myc* expression by S2T1-6OTD may not be the only mechanism explaining the G_0-G_1 arrest of the cell cycle and the cell growth inhibition, but the expression level of other oncogenes may be affected with an effect on downstream signaling pathways governing cell proliferation.

Many experimental lines of evidence from different groups have shown the association of *c-Myc* and cell proliferation (69, 76). We therefore expected that S2T1-6OTD treatments would induce a *c-Myc*–dependent cell growth arrest. Indeed, short-term treatments with S2T1-6OTD induced a dose- and time-dependent negative effect on cell viability of all the MB- and AT/RT-derived cell lines tested already at concentrations lower than 1 μmol/L. Of considerable interest was the finding that S2T1-6OTD showed a significantly lower antiproliferative effect when applied to normal human fibroblast cells MRC-5 (77). Ideally, a *c-Myc*–targeted therapy should be active on cells with deregulated *c-Myc* and should not affect the majority of the normal cells *in vivo*. Here, we showed a more prominent effect of S2T1-6OTD on cellular growth of MB- and AT/RT-derived cells compared with its weaker effects on normal cells, which would be supportive of a selective activity on neoplastic cells.

Treatment with S2T1-6OTD resulted not only in *c-Myc* downregulation but also in a decrease in *hTERT* mRNA and reduction of telomerase activity in most of the cell lines tested. This is of particular interest considering that the catalytic subunit of telomerase *hTERT* is transcriptionally regulated by *c-Myc* (27, 78) and that activation or repression of *c-Myc* can alter hTERT activity in normal or tumor cells both *in vitro* and *in vivo* (22, 28, 79–82). However, on the other hand, our finding that S2T1-6OTD binds more potently to the *c-Myc* promoter sequence did not exclude a weaker binding to telomeric DNA (with 35-fold less efficiency). Together with our discovery that S2T1-6OTD exerted a direct inhibitory effect on TRAP activity in a cell-free system, this result suggests a possible direct inhibition of the telomerase enzyme by S2T1-6OTD and could provide an explanation for the differences between the levels of *c-Myc* activity inhibition and the degree of hTERT activity reduction we observed in Fig. 4. Nevertheless, one should remember that S2T1-6OTD showed a dose- and time-dependent antiproliferative effect on the telomerase-negative human foreskin fibroblast cells (BJ) and on the ALT-dependent D425 while having no antiproliferative effect on *c-Myc* knockout (−/−) HO15.19 rat fibroblast cells or PC12 cells, which do not depend on *c-Myc* in their proliferation. Together, these data confirm that a functional *c-Myc* pathway, and not telomerase, is needed for S2T1-6OTD to exert its antiproliferative effect. This observation counters the concern about the specificity of S2T1-6OTD toward *c-Myc* and reveals that it is *c-Myc* inhibition rather than telomerase downregulation that is responsible for the proliferation arrest exerted by S2T1-6OTD in our experiments.

To extend our findings beyond the outcome of 72-hour treatment, we studied the effects of long-term treatment of MB and AT/RT cells with nontoxic concentrations of S2T1-6OTD, compatible with long-term drug dosage, and observed the effect of telomerase inhibition on the children's brain cancer cells. The desired effect of telomerase inhibition would be to shorten telomeres to critical lengths, causing replicative senescence and preferably cell death. The data obtained from our experiments showed that prolonged treatment did indeed result in a time-dependent telomere shortening that was preceded by a decrease in telomerase activity and accompanied by cell growth arrest and senescence-associated morphologic changes in MB and AT/RT cells, which also showed positive expression of senescence-associated markers. This finding was followed by apoptosis at day 35 in all cells treated.

In conclusion, we have shown the preferential recognition of the G-rich sequence in the *c-Myc* promoter over the telomere sequence by a novel small-molecule S2T1-6OTD. Through its ability to recognize and stabilize a G-quadruplex structure in the *c-Myc* promoter sequence, S2T1-6OTD was able to inhibit *c-Myc* and decrease telomerase activities, to disrupt telomere maintenance, to force cells into senescence, and to induce growth arrest and apoptosis in childhood brain tumor cell lines. A better knowledge about the *in vivo* pharmacokinetics and efficacy of S2T1-6OTD is mandatory. However, S2T1-6OTD may well represent a potential effective and innovative therapeutic strategy for childhood brain tumors.

Disclosure of Potential Conflicts of Interest

No potential conflicts of interest were disclosed.

Acknowledgments

Grant Support

References

1. Rood BR, Macdonald TJ, Packer RJ. Current treatment of medulloblastoma: recent advances and future challenges. Semin Oncol 2004;31:666–75.

2. Rorke LB, Packer RJ, Biegel JA. Central nervous system atypical teratoid/rhabdoid tumors of infancy and childhood: definition of an entity. J Neurosurg 1996;85:56–65.

3. MacDonald TJ, Rood BR, Santi MR, et al. Advances in the diagnosis, molecular genetics, and treatment of pediatric embryonal CNS tumors. Oncologist 2003;8:174–86.

4. Judkins AR, Mauger J, Ht A, et al. Immunohistochemical analysis of hSNF5/INI1 in pediatric CNS neoplasms. Am J Surg Pathol 2004;28:644–50.

5. Biegel JA, Tan L, Zhang F, et al. Alterations of the hSNF5/INI1 gene in central nervous system atypical teratoid/rhabdoid tumors and renal and extrarenal rhabdoid tumors. Clin Cancer Res 2002;8:3461–7.

6. Burger PC, Yu IT, Tihan T, et al. Atypical teratoid/rhabdoid tumor of the central nervous system: a highly malignant tumor of infancy and childhood frequently mistaken for medulloblastoma: a Pediatric Oncology Group study. Am J Surg Pathol 1998;22:1083–92.

7. Bambakidis NC, Robinson S, Cohen M, et al. Atypical teratoid/rhabdoid tumors of the central nervous system: clinical, radiographic and pathologic features. Pediatr Neurosurg 2002;37:64–70.

8. Hilden JM, Meerbaum S, Burger P, et al. Central nervous system atypical teratoid/rhabdoid tumor: results of therapy in children enrolled in a registry. J Clin Oncol 2004;22:2877–84.

9. Tekautz TM, Fuller CE, Blaney S, et al. Atypical teratoid/rhabdoid tumors (ATRT): improved survival in children 3 years of age and older with radiation therapy and high-dose alkylator-based chemotherapy. J Clin Oncol 2005;23:1491–9.

10. Shin-ya K, Wierzba K, Matsuo K, et al. Telomestatin, a novel telomerase inhibitor from Streptomyces anulatus. J Am Chem Soc 2001;123:1262–3.

11. Tahara H, Shin-Ya K, Seimiya H, et al. G-Quadruplex stabilization by telomestatin induces TRF2 protein dissociation from telomeres and anaphase bridge formation accompanied by loss of the 3′ telomeric overhang in cancer cells. Oncogene 2006;25:1955–66.

12. Shammas MA, Reis RJ, Li C, et al. Telomerase inhibition and cell growth arrest after telomestatin treatment in multiple myeloma. Clin Cancer Res 2004;10:770–6.

13. Tauchi T, Shin-Ya K, Sashida G, et al. Activity of a novel G-quadruplex-interactive telomerase inhibitor, telomestatin (SOT-095), against human leukemia cells: involvement of ATM-dependent DNA damage response pathways. Oncogene 2003;22:5338–47.

14. Binz N, Shalaby T, Rivera P, et al. Telomerase inhibition, telomere shortening, cell growth suppression and induction of apoptosis by telomestatin in childhood neuroblastoma cells. Eur J Cancer 2005;41:2873–81.

15. Tera M, Iida K, Ishizuka H, et al. Synthesis of a potent G-quadruplex-binding macrocyclic heptaoxazole. Chembiochem 2009;10:431–5.

16. Kim MY, Vankayalapati H, Shin-Ya K, et al. Telomestatin, a potent telomerase inhibitor that interacts quite specifically with the human telomeric intramolecular G-quadruplex. J Am Chem Soc 2002;124:2098–9.

17. Siddiqui-Jain A, Grand CL, Bearss DJ, et al. Direct evidence for a G-quadruplex in a promoter region and its targeting with a small molecule to repress c-MYC transcription. Proc Natl Acad Sci U S A 2002;99:11593–8.

18. Siebenlist U, Hennighausen L, Battey J, et al. Chromatin structure and protein binding in the putative regulatory region of the c-myc gene in Burkitt lymphoma. Cell 1984;37:381–91.

19. Cooney M, Czernuszewicz G, Postel EH, et al. Site-specific oligonucleotide binding represses transcription of the human c-myc gene in vitro. Science 1988;241:456–9.

20. Davis TL, Firulli AB, Kinniburgh AJ. Ribonucleoprotein and protein factors bind to an H-DNA-forming c-myc DNA element: possible regulators of the c-myc gene. Proc Natl Acad Sci U S A 1989;86:9682–6.

21. Berberich SJ, Postel EH. PuF/NM23-H2/NDPK-B transactivates a human c-myc promoter-CAT gene via a functional nuclease hypersensitive element. Oncogene 1995;10:2343–7.

22. Grand CL, Han H, Munoz RM, et al. The cationic porphyrin TMPyP4 down-regulates c-MYC and human telomerase reverse transcriptase expression and inhibits tumor growth in vivo. Mol Cancer Ther 2002;1:565–73.

23. Hurley LH, Von Hoff DD, Siddiqui-Jain A, et al. Drug targeting of the c-MYC promoter to repress gene expression via a G-quadruplex silencer element. Semin Oncol 2006;33:498–512.

24. Obaya AJ, Mateyak MK, Sedivy JM. Mysterious liaisons: the relationship between c-Myc and the cell cycle. Oncogene 1999;18:2934–41.

25. Schmidt EV. The role of c-myc in cellular growth control. Oncogene 1999;18:2988–96.

26. Trumpp A, Refaeli Y, Oskarsson T, et al. c-Myc regulates mammalian body size by controlling cell number but not cell size. Nature 2001;414:768–73.

27. Wang J, Xie LY, Allan S, et al. Myc activates telomerase. Genes Dev 1998;12:1769–74.

28. Wu KJ, Grandori C, Amacker M, et al. Direct activation of TERT transcription by c-MYC. Nat Genet 1999;21:220–4.

29. Felsher DW, Bishop JM. Reversible tumorigenesis by MYC in hematopoietic lineages. Mol Cell 1999;4:199–207.

30. Shachaf CM, Kopelman AM, Arvanitis C, et al. MYC inactivation uncovers pluripotent differentiation and tumour dormancy in hepatocellular cancer. Nature 2004;431:1112–7.

31. D'Cruz CM, Gunther EJ, Boxer RB, et al. c-MYC induces mammary tumorigenesis by means of a preferred pathway involving spontaneous Kras2 mutations. Nat Med 2001;7:235–9.

32. Arnold I, Watt FM. c-Myc activation in transgenic mouse epidermis results in mobilization of stem cells and differentiation of their progeny. Curr Biol 2001;11:558–68.

33. Grotzer MA, Castelletti D, Fiaschetti G, et al. Targeting Myc in pediatric malignancies of the central and peripheral nervous system. Curr Cancer Drug Targets 2009;9:176–88.

34. Scheurlen WG, Schwabe GC, Joos S, et al. Molecular analysis of childhood primitive neuroectodermal tumors defines markers associated with poor outcome. J Clin Oncol 1998;16:2478–85.

35. Badiali M, Pession A, Basso G, et al. N-myc and c-myc oncogenes amplification in medulloblastomas. Evidence of particularly aggressive behavior of a tumor with c-myc amplification. Tumori 1991;77:118–21.

36. Herms J, Neidt I, Lüscher B, et al. C-myc expression in medulloblastoma and its prognostic value. Int J Cancer 2000;89:395–402.

37. Grotzer MA, Hogarty MD, Janss AJ, et al. MYC messenger RNA expression predicts survival outcome in childhood primitive neuroectodermal tumor/medulloblastoma. Clin Cancer Res 2001;7:2425–33.

38. Bruggers CS, Tai KF, Murdock T, et al. Expression of the c-Myc protein in childhood medulloblastoma. J Pediatr Hematol Oncol 1998;20:18–25.

39. Bigner SH, Friedman HS, Vogelstein B, et al. Amplification of the c-myc gene in human medulloblastoma cell lines and xenografts. Cancer Res 1990;50:2347–50.

40. Aldosari N, Bigner SH, Burger PC, et al. MYCC and MYCN oncogene amplification in medulloblastoma. A fluorescence *in situ* hybridization study on paraffin sections from the Children's Oncology Group. Arch Pathol Lab Med 2002;126:540–5.

41. Giangaspero F, Rigobello L, Badiali M, et al. Large-cell medulloblastomas: a distinct variant with highly aggressive behavior. Am J Surg Pathol 1992;16:687–93.

42. Eberhart CG, Kratz JE, Schuster A, et al. Comparative genomic hybridization detects an increased number of chromosomal alterations in large cell/anaplastic medulloblastomas. Brain Pathol 2002;12:36–44.

43. Jay V, Squire J, Bayani J, et al. Oncogene amplification in medulloblastoma: analysis of a case by comparative genomic hybridization and fluorescence *in situ* hybridization. Pathology 1999;31:337–44.

44. Eberhart CG, Kratz J, Wang Y, et al. Histopathological and molecular prognostic markers in medulloblastoma: c-myc, N-myc, TrkC, and anaplasia. J Neuropathol Exp Neurol 2004;63:441–9.

45. Stearns D, Chaudhry A, Abel TW, et al. c-myc overexpression causes anaplasia in medulloblastoma. Cancer Res 2006;66:673–81.

46. Tera M, Ishizuka H, Takagi M, et al. Macrocyclic hexaoxazoles as sequence- and mode-selective G-quadruplex binders. Angew Chem Int Ed Engl 2008;47:5557–60.

47. Didiano D, Shalaby T, Lang D, et al. Telomere maintenance in childhood primitive neuroectodermal brain tumors. Neuro-oncol 2004;6:1–8.

48. Kunz F, Shalaby T, Lang D, et al. Quantitative mRNA expression analysis of neurotrophin-receptor TrkC and oncogene c-MYC from formalin-fixed, paraffin-embedded primitive neuroectodermal tumor samples. Neuropathology 2006;26:393–9.

49. von Bueren AO, Shalaby T, Rajtarova J, et al. Anti-proliferative activity of the quassinoid NBT-272 in childhood medulloblastoma cells. BMC Cancer 2007;7:19.

50. Sharma-Walia N, Krishnan HH, Naranatt PP, et al. ERK1/2 and MEK1/2 induced by Kaposi's sarcoma-associated herpesvirus (human herpesvirus 8) early during infection of target cells are essential for expression of viral genes and for establishment of infection. J Virol 2005;79:10308–29.

51. Riou JF, Guittat L, Mailliet P, et al. Cell senescence and telomere shortening induced by a new series of specific G-quadruplex DNA ligands. Proc Natl Acad Sci U S A 2002;99:2672–7.

52. Grotzer MA, Janss AJ, Fung K, et al. TrkC expression predicts good clinical outcome in primitive neuroectodermal brain tumors. J Clin Oncol 2000;18:1027–35.

53. Grotzer MA, Janss AJ, Phillips PC, et al. Neurotrophin receptor TrkC predicts good clinical outcome in medulloblastoma and other primitive neuroectodermal brain tumors. Klin Padiatr 2000;212:196–9.

54. Lemarteleur T, Gomez D, Paterski R, et al. Stabilization of the c-myc gene promoter quadruplex by specific ligands' inhibitors of telomerase. Biochem Biophys Res Commun 2004;323:802–8.

55. Freyer MW, Buscaglia R, Kaplan K, et al. Biophysical studies of the c-MYC NHE III1 promoter: model quadruplex interactions with a cationic porphyrin. Biophys J 2007;92:2007–15.

56. Seenisamy J, Rezler EM, Powell TJ, et al. The dynamic character of the G-quadruplex element in the c-MYC promoter and modification by TMPyP4. J Am Chem Soc 2004;126:8702–9.

57. Sanchez-Ruiz JM. Ligand effects on protein thermodynamic stability. Biophys Chem 2007;126:43–9.

58. Reed J, Gunaratnam M, Beltran M, et al. TRAP-LIG, a modified telomere repeat amplification protocol assay to quantitate telomerase inhibition by small molecules. Anal Biochem 2008;380:99–105.

59. Facchini LM, Penn LZ. The molecular role of Myc in growth and transformation: recent discoveries lead to new insights. FASEB J 1998;12:633–51.

60. Simonsson T, Henriksson M. c-myc suppression in Burkitt's lymphoma cells. Biochem Biophys Res Commun 2002;290:11–5.

61. Mateyak MK, Obaya AJ, Adachi S, et al. Phenotypes of c-Myc-deficient rat fibroblasts isolated by targeted homologous recombination. Cell Growth Differ 1997;8:1039–48.

62. Hopewell R, Ziff EB. The nerve growth factor-responsive PC12 cell line does not express the Myc dimerization partner Max. Mol Cell Biol 1995;15:3470–8.

63. Jacobs JP, Jones CM, Baille JP. Characteristics of a human diploid cell designated MRC-5. Nature 1970;227:168–70.

64. Zhu H, Gooderham N. Neoplastic transformation of human lung fibroblast MRC-5 SV2 cells induced by benzo[a]pyrene and confluence culture. Cancer Res 2002;62:4605–9.

65. Bodnar AG, Ouelette M, Frolkis M, et al. Extension of life-span by introduction of telomerase into normal human cells. Science 1998;279:349–52.

66. Dexheimer TS, Carey SS, Zuohe S, et al. NM23-H2 may play an indirect role in transcriptional activation of c-myc gene expression but does not cleave the nuclease hypersensitive element III1. Mol Cancer Ther 2009;8:1363–77.

67. Huppert JL, Balasubramanian S. G-quadruplexes in promoters throughout the human genome. Nucleic Acids Res 2007;35:406–13.

68. Gonzalez V, Guo K, Hurley L, Sun D. Identification and characterization of nucleolin as a c-myc G-quadruplex-binding protein. J Biol Chem 2009;284:23622–35.

69. Rovera G, Olashaw N, Meo P. Terminal differentiation in human promyelocytic leukaemic cells in the absence of DNA synthesis. Nature 1980;284:69–70.

70. Westin EH, Wong-Staal F, Gelmann EP, et al. Expression of cellular homologues of retroviral onc genes in human hematopoietic cells. Proc Natl Acad Sci U S A 1982;79:2490–4.

71. Grosso LE, Pitot HC. Modulation of c-myc expression in the HL-60 cell line. Biochem Biophys Res Commun 1984;119:473–80.

72. Reitsma PH, Rothberg PG, Astrin SM, et al. Regulation of myc gene expression in HL-60 leukaemia cells by a vitamin D metabolite. Nature 1983;306:492–4.

73. Marampon F, Ciccarelli C, Zani BM. Down-regulation of c-Myc following MEK/ERK inhibition halts the expression of malignant phenotype in rhabdomyosarcoma and in non muscle-derived human tumors. Mol Cancer 2006;5:31.

74. Kim YH, Buchholz MA, Chrest FJ, et al. Up-regulation of c-myc induces the gene expression of the murine homologues of p34cdc2 and cyclin-dependent kinase-2 in T lymphocytes. J Immunol 1994;152:4328–35.

75. Abaza MS, Al-Saffar A, Al-Sawan S, et al. c-myc antisense oligonucleotides sensitize human colorectal cancer cells to chemotherapeutic drugs. Tumour Biol 2008;29:287–303.

76. Einat M, Resnitzky D, Kimchi A. Close link between reduction of c-myc expression by interferon and G_0/G_1 arrest. Nature 1985;313:597–600.

77. Waters CM, Littlewood TD, Hancock DC, et al. c-myc protein expression in untransformed fibroblasts. Oncogene 1991;6:797–805.

78. Hahn WC, Meyerson M. Telomerase activation, cellular immortalization and cancer. Ann Med 2001;33:123–9.

79. Oh S, Song YH, Kim UJ, et al. *In vivo* and *in vitro* analyses of Myc for differential promoter activities of the human telomerase (hTERT) gene in normal and tumor cells. Biochem Biophys Res Commun 1999;263:361–5.

80. Hao H, Nancai Y, Lei F, et al. siRNA directed against c-Myc inhibits proliferation and downregulates human telomerase reverse transcriptase in human colon cancer Colo 320 cells. J Exp Clin Cancer Res 2008;27:27.

81. Greenberg RA, O'Hagan RC, Deng H, et al. Telomerase reverse transcriptase gene is a direct target of c-Myc but is not functionally equivalent in cellular transformation. Oncogene 1999;18:1219–26.

82. Kyo S, Takakura M, Taira T, et al. Sp1 cooperates with c-Myc to activate transcription of the human telomerase reverse transcriptase gene (hTERT). Nucleic Acids Res 2000;28:669–77.

Molecular Cancer Therapeutics

Disabling *c-Myc* in Childhood Medulloblastoma and Atypical Teratoid/Rhabdoid Tumor Cells by the Potent G-Quadruplex Interactive Agent S2T1-6OTD

Tarek Shalaby, André O. von Bueren, Marie-Louise Hürlimann, et al.

Updated version	Access the most recent version of this article at: doi:10.1158/1535-7163.MCT-09-0586
Supplementary Material	Access the most recent supplemental material at: http://mct.aacrjournals.org/content/suppl/2010/01/06/1535-7163.MCT-09-0586.DC1

Cited articles	This article cites 82 articles, 25 of which you can access for free at: http://mct.aacrjournals.org/content/9/1/167.full#ref-list-1
Citing articles	This article has been cited by 2 HighWire-hosted articles. Access the articles at: http://mct.aacrjournals.org/content/9/1/167.full#related-urls

E-mail alerts	Sign up to receive free email-alerts related to this article or journal.
Reprints and Subscriptions	To order reprints of this article or to subscribe to the journal, contact the AACR Publications Department at pubs@aacr.org.
Permissions	To request permission to re-use all or part of this article, use this link http://mct.aacrjournals.org/content/9/1/167. Click on "Request Permissions" which will take you to the Copyright Clearance Center's (CCC) Rightslink site.